JOURNAL OF APPLIED ELECTROCHEMISTRY 11 (1981) 453–461

Effects of ionic migration on the concentrations and mass transfer rate in the diffusion layer of dissolving metals

B. G. ATEYA

Chemistry Department, Faculty of Science, Cairo University, Cairo, Egypt

H. W. PICKERING

Metallurgy Section, Materials Science and Engineering Department, The Pennsylvania State University, University Park, Pennsylvania, USA

Received 28 August 1980

The transport processes occurring within the diffusion layer of dissolving anodes are analysed with the help of a mathematical model which takes into account mass transfer by both diffusion and ionic migration in the presence of a supporting electrolyte. The steady-state transport equations are solved for the ionic concentrations and potential difference as a function of distance within the diffusion layer, metal-ion charge and diffusivity, supporting electrolyte concentration and metal dissolution rate. Upon normalization of the variables, a dimensionless group ($I = ix/zFc^0 D_{M^{z+}}$) is obtained. This group includes the transport properties of the system and shows the inter-relationship between them. The anodic dissolution of Cu in $HClO_4$ was chosen to test some of the predictions of the system. The measured metal-ion concentrations were much less, while the potential gradient was much higher, than predicted. This is explained on the basis of ionic interactions which operate at higher concentrations. It is shown, both theoretically and experimentally, that in this strong acid medium the concentration of hydrogen ions decreases in the diffusion layer of a dissolving anode due to ionic migration of the hydrogen ions in accord with the prevailing potential gradient.

1. Introduction

The question of ionic migration is of fundamental importance in treating mass transfer in electrochemical systems. Its importance was recognized in the early works of Brunner, Eucken and Baars for the electrodeposition of metals; these works are reviewed by Vetter [1]. It was established therein that if the initial concentration of the discharging ion is much less than that of the supporting electrolyte, ionic migration effects may be neglected and the current becomes essentially a diffusion current. On the other hand, in the absence of a supporting electrolyte, ionic migration increases the limiting currency i_L to $i_L(1 + Z)$ where Z is the ratio of the cation valency to that of the anion. Levich [2] and, subsequently, Newman [3] presented treatments similar to those of Eucken and arrived at the same conclusions. Newman [4] has subsequently treated the effect of ionic migration on the limiting current of an electrodeposition reaction for various hydrodynamic conditions. The effect of ionic migration on the overall rate of mass transfer below the limiting current has not been demonstrated in these treatments. Furthermore, the effect of ionic migration under conditions of anodic dissolution cannot be evaluated on the basis of the existing treatments of a deposition process, since the ratio of metal ion to supporting electrolyte concentration cannot be determined beforehand.

In either deposition or dissolution, an important consideration is the above-mentioned variation of the metal ion/supporting ion concentration ratio. Since this ratio may vary considerably with distance from the electrode surface, ionic migration may, correspondingly, be significant or negligible. Concentration profiles are also important, since they generate density differences which could lead to natural convection.

This paper is concerned with metal dissolution reactions. Its objectives are:

0021–891X/81/040453–09$02.90/0

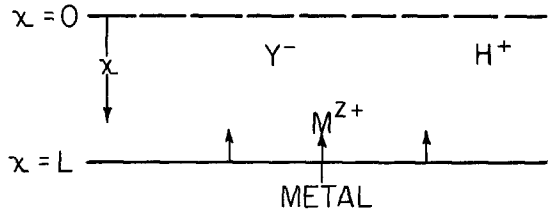

Fig. 1. Geometrical representation of the one-dimensional dissolution–transport model.

(a) To evaluate the relative contributions of ionic migration and molecular diffusion to the overall rate of mass transfer under various conditions of supporting electrolyte concentrations (c^0), metal dissolution current (i), metal ion diffusivity ($D_{M^{z+}}$), and charge on the metal ion (z).

(b) To calculate the profiles of the electrical potential difference and of the various ionic concentrations, including those of the supporting electrolyte in the diffusion layer, to illustrate the effect of such concentration variations on the electrolyte resistivity and to show the relevance of the results to the study of the kinetics of metal dissolution reactions.

(c) To compare the predictions of the model with the experimental results obtained on a selected system.

2. Model, assumptions and solutions

2.1. *Physical model and assumptions*

Consider a metal which dissolves in a strong acid HY (supporting electrolyte) according to the reaction

$$M \rightarrow M^{z+} + ze. \tag{1}$$

The acid is assumed to be strong enough to prevent the hydrolysis of the metal ion M^{z+}; Y^- is a noncomplexing ligand. The transport processes at a planar surface are assumed to be one-dimensional and only migration and diffusion are considered (Fig. 1). This geometry is quite similar to those existing in experiments on metal dissolution kinetics [5–12] or on electropolishing of metals [13]. These same transport conditions also apply to special cases of pitting or cracking [14]. The rate of mass transfer is the sum of the rates of ionic diffusion, given by Fick's law, and of ionic migration, with the ionic mobility given by the Nernst–Einstein relation between ionic mobility μ_i and molecular diffusivity D_i, $\mu_i = (F/RT)D_i$, where F is the Faraday constant, R the gas constant and T the absolute temperature. At steady state, the fluxes of the various ionic species are given by:

$$J_{H^+} = -D_{H^+}\left[\frac{dc_{H^+}}{dx} + c_{H^+}\frac{T}{RT}\frac{d\Phi}{dx}\right] = 0 \tag{2}$$

$$J_{Y^-} = -D_{Y^-}\left[\frac{dc_{Y^-}}{dx} - c_{Y^-}\frac{F}{RT}\frac{d\Phi}{dx}\right] = 0 \tag{3}$$

$$J_{M^{z+}} = -D_{M^{z+}}\left[\frac{dc_{M^{z+}}}{dx} + zc_{M^{z+}}\frac{F}{RT}\frac{d\Phi}{dx}\right] = -\frac{i}{zF} \tag{4}$$

where Φ is the electrical potential difference in the electrolyte ($\Phi = 0$ at $x = 0$, see the boundary conditions in Equation 6), i is the anodic dissolution rate and c refers to ionic concentrations. The fluxes of H^+ and Y^- ions are zero, as shown in Equations 2 and 3, since they are neither formed nor consumed by the electrode reaction. The right-hand side of Equation 4 has a negative sign since metal ions move in the direction of decreasing value of the x co-ordinate. The assumption of electroneutrality requires that

$$c_{H^+} + zc_{M^{z+}} = c_{Y^-}. \tag{5}$$

The boundary conditions at $x = 0$ are

$$c_{M^{z+}} = 0 \tag{6a}$$

$$\Phi = 0 \tag{6b}$$

$$c_{H^+} = c_{Y^-} = c^0. \tag{6c}$$

Equation 6c follows from Equation 6a and the electroneutrality condition of Equation 5. The plane $x = 0$ is the outer plane of the diffusion layer in a large container with enough stirring beyond this layer to keep $c_{M^{z+}} = 0$. Equations 2–6 are sufficient to calculate c_{H^+}, c_{Y^-}, $c_{M^{z+}}$ and Φ as a function of $x, i, z \ldots$ etc.

2.2. *Analytical solutions*

Dividing Equations 2, 3 and 4 by D_{H^+}, D_{Y^-} and $D_{M^{z+}}$, respectively, adding, using Equation 5 and integrating using Equation 6, one obtains

$$\bar{c}_{H^+} + \bar{c}_{Y^-} + \bar{c}_{M^{z+}} = I + 2 \tag{7}$$

where

$$I = (ix/zFc^0D_{M^{z+}})$$

and the dimensionless concentrations are given by

$$\bar{c}_{H^+} = c_{H^+}/c^0, \qquad \bar{c}_{Y^-} = c_{Y^-}/c^0$$

$$\text{and} \qquad \bar{c}_{M^{z+}} = c_{M^{z+}}/c^0.$$

The bars will be dropped for convenience, and it is to be understood that all the concentrations are dimensionless.

The dimensionless parameter $I = ix/zFc^0D_{M^{z+}}$ includes all the transport properties of the system. The implication here is that the net value of I (rather than the separate values of i, x, c^0 or $D_{M^{z+}}$) is the controlling factor. Thus an increase in x or i has the same effect on the potential difference Φ or the ionic concentrations as an equivalent decrease in $D_{M^{z+}}$ or c^0. With the exception of z, the above variables occur only in I, as shown below in obtaining the solutions. Consequently, the values of I and z determine the corresponding potential difference and ionic concentrations (cf. Equation 9). Equations 2 and 3 can be solved, then combined with Equation 6 to give

$$c_{H^+} = 1/c_{Y^-}. \tag{8}$$

The solution of Equations 5 and 7 for c_{Y^-} gives rise to

$$c_{Y^-} = (1/2)[I + 2 + (z-1)c_{M^{z+}}]. \tag{9}$$

The relation between c_{H^+} and $c_{M^{z+}}$ is obtained by combining Equations 8 and 9. Thus,

$$c_{H^+} = \frac{2}{I + 2 + (z-1)c_{M^{z+}}}. \tag{10}$$

Substituting Equations 9 and 10 in Equation 7 and solving for $c_{M^{z+}}$ one gets

$$(z^2-1)c^2_{M^{z+}} + 2(I+2)c_{M^{z+}} - [I^2 + 4I] = 0. \tag{11}$$

This is a quadratic equation in $c_{M^{z+}}$, the positive root of which is given by Equation 12 after several algebraic steps:

$$c_{M^{z+}} = \frac{-(I+2) + [z^2(I^2+4I)+4]^{1/2}}{z^2-1}. \tag{12}$$

Once $c_{M^{z+}}$ is obtained from Equation 12, c_{Y^-} and c_{H^+} can be calculated from Equations 9 and 10, respectively.

A solution for Φ is obtained by integrating Equation 2 or Equation 3 and using Equation 6b as a boundary condition. Thus

$$\Phi = \frac{2.303\,RT}{F}\log(c_{Y^-}). \tag{13}$$

For any value of the ionic charge z, the solutions obtained satisfy the original differential equations and the boundary conditions in Equation 6, i.e., at $x = 0$, $c_{M^{z+}} = 0$, $c_{Y^-} = c^\circ$ and $\Phi = 0$.

3. Discussion of the model predictions

3.1. *Variations of ionic concentrations*

As the above solutions show, the value of I determines the potential difference and the ionic concentrations, and is itself determined by the five different parameters and variables of the system, i, x, z, c^0 and $D_{M^{z+}}$. The dependence of the electrical potential and the normalized ionic concentrations on I and z is shown in Fig. 2.

The ionic concentrations in Fig. 2 are in multiples of the bulk electrolyte concentration c^0 and the abscissa is I. Thus, for certain values of i, z, c^0 and $D_{M^{z+}}$, the plots give the profiles of ionic concentrations in the diffusion layer in multiples of c^0. The actual value of concentration is the product of the value on the curves times c^0. The concentrations of the various ionic species at the metal

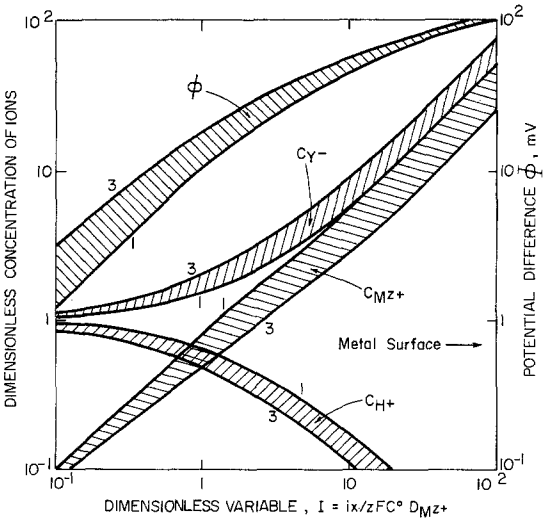

Fig. 2. Effect of the dimensionless variable I on the potential difference Φ and on the dimensionless ionic concentrations for various values of metal ion charge z. The numbers on each curve refer to z.

surface are obtained by substituting δ for x, where δ is the diffusion layer thickness.

Results in Fig. 2 define the conditions under which the ionic concentrations at the metal surface are significantly different from the bulk values. Clearly, below a value of $I = 0.1/z$, the ionic concentrations and potential difference Φ are essentially equal to the bulk values. For the common case of iron dissolution in acid chloride media, the value $I = 0.1/z$ corresponds to a current of 1 mA cm^{-2} (taking x to be the diffusion layer thickness $\delta = 0.05$ cm, $D = 5 \times 10^{-6}$ cm^2 s^{-1} [15], $c^0 = 10^{-3}$ mol cm^{-3} and $z = 2$). Thus, under these conditions the concentrations of H^+ and Y^- ions at the metal surface are equal to their bulk values. At larger values of I, the anion and metal ion concentrations at the metal surface increase, whereas c_{H^+} decreases. The magnitude of these departures from the bulk composition depends on I and z, as shown in Fig. 2; it may be several-fold, or an order of magnitude or more, depending on the values of i, z, c^0, $D_{M^{z+}}$ and x. The extent of agreement between these predicted concentrations, in which negligible ionic interactions are assumed, and actual concentrations is shown below.

One area in which the results of the present work may be used with advantage is the kinetics of metal dissolution, where mechanisms are developed on the basis of reaction-order studies using bulk concentrations of ions, e.g., H^+ and Cl^- ions [5–12]†. As shown above, the surface concentrations are predicted to be significantly different from the bulk values for $I > 0.1/z$, and hence the 'as-calculated' reaction orders for this condition are of questionable value. It remains to be seen, however, whether reaction orders obtained by using the above calculated surface concentrations are more meaningful for the analysis of reaction mechanisms than those obtained by restricting the use of bulk values to those conditions for which $I \lesssim 0.1/z$.

From the above results one can also predict the conditions under which the onset of precipitation of metal salts occurs on the surface of dissolving metals for comparison with experimental results. Such salt films have been shown to control the electropolishing of copper in phosphoric acid [13].

Another area of application is localized corrosion where a similar modelling approach proved useful in understanding the mechanisms involved in pitting, crevice and cracking corrosion [14, 16, 17]. Results of the present work extend the earlier quantitative treatments of pitting corrosion [14] to $z > 1$.

† Many of these references have extensive literature reviews.

3.2. *Variations of resistivity*

At any value of I, the total concentration of ions is greater than the bulk value, with the highest concentration occurring for $z = 1$. Consequently, the local resistivity in the diffusion layer decreases as the surface is approached. The resistivity ρ of an electrolyte is given by

$$\rho = \frac{1}{F \sum_i z_i^2 \mu_i c_i}. \tag{14}$$

Substituting for μ_i by the Nernst–Einstein relation, one obtains

$$\rho = \frac{RT}{F^2} \sum_i \frac{1}{D_i z_i^2 c_i}. \tag{15}$$

The dimensionless resistivity, which is the ratio of the local to bulk electrolyte resistivities is given by

$$\bar{\rho}(I) = \frac{\rho(x)}{\rho(x=0)} = \frac{\Sigma_i D_i z_i^2 c_i \text{ (bulk electrolyte)}}{\Sigma_i D_i z_i^2 c_i \text{ (in diffusion layer)}}. \tag{16}$$

Though Equations 14 and 15 are applicable only for dilute solutions and are without regard for diffusion potentials, they do illustrate the resistivity variations. These variations are schematically shown in Fig. 3 for $z = 1$, 2 and 3 assuming equal diffusivities for all ions. For $I < 0.01$, $\bar{\rho}(I)$ approaches unity independent of z. At larger values of I, $\bar{\rho}$ decreases with the lowest resistivity corresponding to $z = 3$. These results are in general agreement with previous work on pitting [18, 19] where resistivity variations have been predicted using basically different modelling approaches.

3.3. *Ionic migration versus diffusive fluxes*

This section compares the ratio (R) of the ionic migration and diffusion fluxes in order to define the ranges of current, distance, ionic charge and bulk electrolyte concentration for which ionic migration may or may not be ignored. From the solutions presented above, the metal ion fluxes

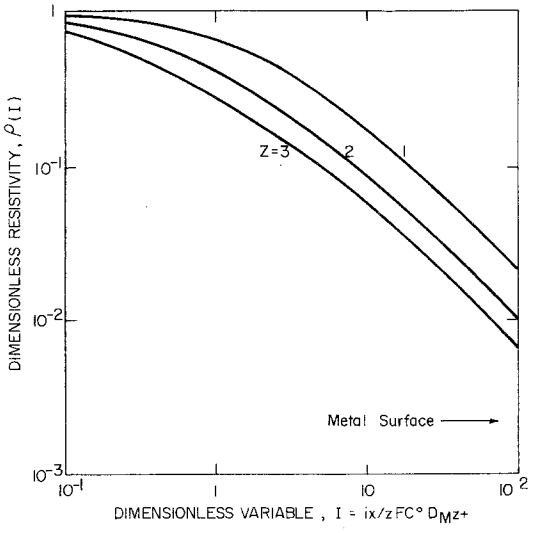

Fig. 3. Effect of the dimensionless variable I on the dimensionless resistivity (Equation 16) for various values of metal ion charge z.

are given as follows†: For $z = 1$

$$\text{Diffusion flux} = -D\frac{dc}{dx} = \frac{i^2x/F - iD(c - 2c^0)}{2c^0FD + ix} \quad (17)$$

$$\text{Migration flux} = Dc\frac{F}{RT}\frac{d\Phi}{dx} = \frac{Dci}{ix + 2c^0FD}. \quad (18)$$

For $z > 1$

$$\text{Diffusive flux} = \frac{1}{z^2 - 1} \times \left[\frac{i}{zF} - \frac{i^2x/F^2D + 2zic^0/F}{\{[(ix/FD)^2 + 4zi(xc^0/FD) + 4c^0]^{1/2}\}}\right] \quad (19)$$

$$\text{Migration flux} = -zDc\left[\frac{i/zFD + (z-1)dc/dx}{ix/zFD + 2c^0 + (z-1)c}\right]. \quad (20)$$

The ratio of ionic migration to diffusive fluxes R, at various conditions of i, x, z and c^0, was calcalculated using Equations 17–20 for $z = 1, 2$ and 3. The results in Fig. 4 show that the ratio of ionic

† For convenience, D and c refer to the diffusivity and concentration of metal ions in this section only.

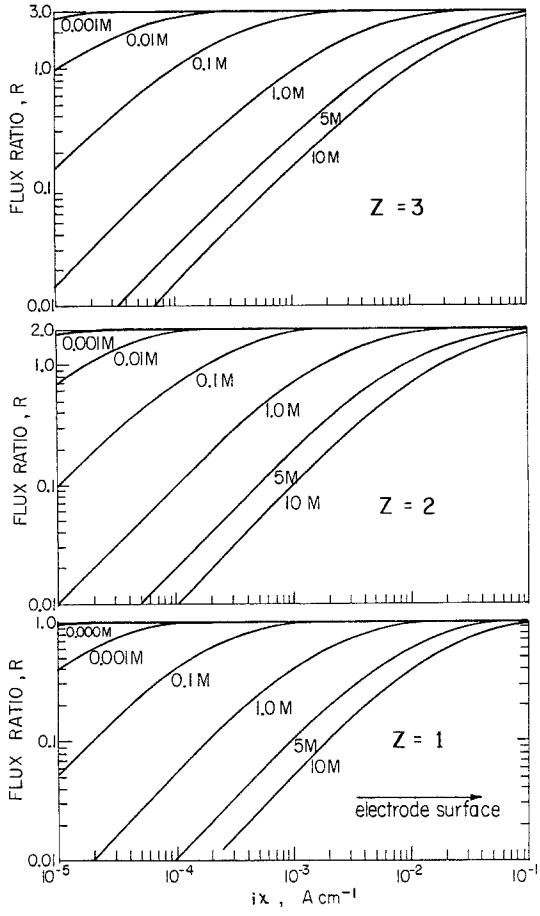

Fig. 4. Variation of the flux ratio R with the product ix for various values of bulk electrolyte concentrations c^0 and metal ion charge z.

migration to diffusive fluxes is determined by three factors:

(a) The product ix. As ix increases, the ratio R increases to a limiting value, R_{lim}.

(b) The bulk electrolyte concentration c^0. An increase in c^0 decreases R, and this trend is greater at lower ix values. Thus R_{lim} is obtained at lower values of ix for lower values of c^0.

(c) The ionic charge z. The values of R and R_{lim} increase with increase in z. One of the significant results of this model is that $R_{\text{lim}} = 1, 2$ and 3 for $z = 1, 2$ and 3, respectively. This, in turn, means that the limiting migration flux is, respectively, one, two or three times as large as the diffusion flux. Consequently, under limiting conditions of ionic migration ($I = ix/zFc^0D_{Mz+} > 10$), the overall rate of mass transfer is two, three or four times the diffusion rate for $z = 1, 2$ and 3,

respectively. On the other hand, ionic migration becomes negligible ($R < 0.1$) for $I < 0.2$ for $z = 1$, $I < 0.05$ for $z = 2$ and $I < 0.025$ for $z = 3$.

4. Experimental

4.1. *Selection of an experimental system*

An ideal experimental system for a quantitative test of the predictions of the above model should meet the following requirements:

(a) The acid is strong, i.e., completely ionized with a stable (non-oxidizable or reducible) monovalent noncomplexing anion. This rules out HCl, HNO_3 and H_2SO_4, and hence $HClO_4$ was chosen.

(b) Upon dissolution, the metal produces an ion with a single valency state which is not susceptible to hydrolysis or complexing.

(c) The diffusion coefficient of the metal ion is independent of its concentration. It must also be known with certainty.

In view of the above, the dissolution of copper in 1 M $HClO_4$ seemed to be the optimum system for our purpose. Although the diffusion of $CuSO_4$ has been studied extensively and its coefficient known to vary considerably with concentration [20], much less is known about the diffusion of $Cu(ClO_4)_2$. However, it is reported [21, 22] that the diffusion coefficient of copper perchlorate is somewhat lower than that of copper sulphate due, possibly, to the formation of copper sulphate complexes.

4.2. *Experimental procedure*

In order to maintain conditions of one-dimensional transport through an artificially large diffusion layer, the test cell shown in Fig. 5 was used. It is similar to other frequently used artificial pits [14, 18, 19]. The bottom part was made of 99.9+% Cu. Electrical contact was made through a thin platinum wire protected from the solution with a tight heat-shrinkable tubing. The cross-sectional area was about 0.3 cm^2. The counter electrode was positioned about 10 cm away from the cell to insure uniform current lines at its opening. The solution was 1 M $HClO_4$ in a 1200 cm^3 container. The large volume keeps $c_{Cu^{2+}} \simeq 0$ in the bulk as required by Equation 6. Though the system was open to air, corrosion of the Cu by oxygen

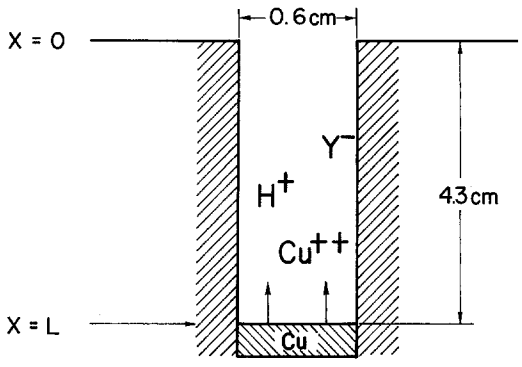

Fig. 5. Illustration of the one-dimensional cell used for the experimental measurements.

reduction was considered negligible in view of the small mass transfer coefficient of oxygen, $m = D/L$ (due to the long diffusion path, L), compared to the impressed dissolution rate. A constant anodic current was impressed on the electrode and the potential between the Luggin probe (0.01 cm diameter) and the metal surface was measured versus an Hg/Hg_2SO_4 reference electrode using a 1 M $HClO_4$ salt bridge.

The concentration of Cu^{2+} was measured as a function of distance using a Cu wire as an ion-selective electrode and a properly constructed calibration curve. The wire was of high-purity copper, the immersed region of which was covered with a heat-shrinkable tubing except for its very end. This gave a tight seal and it was certain the electrolyte solution reached only the tip of the wire. The cross-sectional area of the wire was about one-tenth that of the cell. The calibration curve was constructed using this ion-selective electrode and a set of $Cu(ClO_4)_2$–$HClO_4$ solutions. The copper solutions were prepared by dissolving equivalent amounts of CuO in 71% $HClO_4$ ($\sim$ 11.7 M) and were standardized iodometrically [23]. The $HClO_4$ concentrations were adjusted by simple volumetric dilution. Distilled water ($\rho > 10^5$ ohm cm) was used throughout. All tests were run at room temperature, 25 ± 2° C. The position of either the reference or the ion-selective electrode inside the cell was adjusted, and the distance x measured using a micromanipulator. The potential difference between the Cu surface in the cell and the Luggin capillary of the reference electrode was measured with the latter positioned at various distances inside the cell using a high-

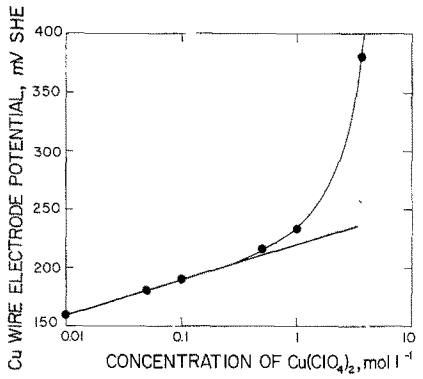

Fig. 6. Calibration curve used to measure the concentration of Cu^{2+} ions (in 1 M $HClO_4$) inside the cell.

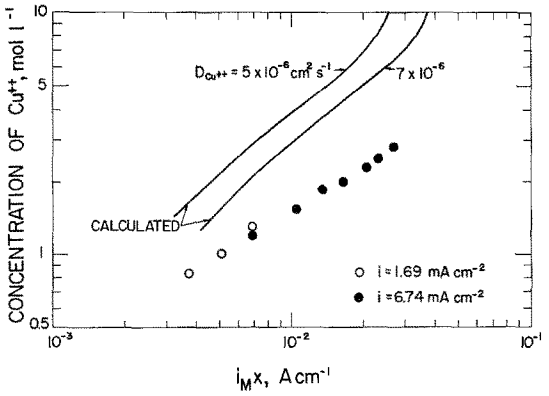

Fig. 7. Comparison of the measured and predicted concencentration of Cu^{2+} inside the cell. Measurements were taken at $x \geqslant 1$ cm.

input impedence voltmeter. The potential difference Φ was calculated from

$$\Phi = E_x - E_{x=0}. \qquad (21)$$

To measure the profile of Cu^{2+} in the cell, it was necessary for the tip of the Luggin capillary to travel along with the ion-selective electrode, such that both were in the same (horizontal) plane normal to the x axis. By this arrangement, no ohmic potential drop was included and only the potential of the Cu-wire ion-selective electrode was measured. The latter potential is a function of the local concentration of Cu^{2+} ions and the ionic strength.

The development of the blue colour of Cu^{2+} ions as a function of time and distance into the cell along with the potential probe and concentration profile measurements were used as indicators of the approach to steady state. Calculation of the rate of recession of the Cu surface by anodic dissolution for the currents used here shows that this rate is several orders of magnitude smaller than the limiting mass transfer coefficient, $m = D/L$. Hence, a steady state can be assumed.

4.3. *Experimental results*

Fig. 6 shows the calibration curve used as a basis for measuring the concentration profile of copper ions in the cell. At low concentrations (and constant ionic strength) the relation is a straight line with a slope of 30 mV, in agreement with the Nernst equation. As the concentration increases, considerable deviation from this behaviour is observed which is attributed to variations in the activity coefficient due to the increase in ionic strength.

The concentration of Cu^{2+} at the top of the cell was found to be about 10^{-3} mol dm^{-3}. This was two orders of magnitude smaller than the measured concentration at 0.5 cm inside the cell, and hence was taken as a satisfactory approximation of the boundary condition (Equation 6).

Fig. 7 shows a comparison between the predicted and the experimental concentration profiles. The data points were for current densities of 1.7 and 6.7 mA cm^{-2}. These points were all obtained at large distances ($x > 1$ cm) in order to eliminate entrance effects, and after steady state was reached. The same results were obtained 2–3 days later. The figure also shows the predicted relations for two values of D, namely 5 and 7×10^{-6} cm^2 s^{-1}. Although the model correctly predicts the shape of the relation, the measured concentrations are significantly lower than the predicted. The figure also shows the effect on the concentration of a 40% increase in the value of D. A good match between the predicted and the measured concentrations is obtainable at a value of D of about 1.8×10^{-5} cm^2 s^{-1}. This is quite a high value, more than twice the value of the diffusion coefficient of Cu^{2+} ions at infinite dilution. We have no reason to believe that the diffusion coefficient of Cu^{2+} in our system is that high. Hence an alternative explanation must be offered.

Fig. 8 shows a comparison between the calculated and the measured values of the potential difference Φ. Again, the agreement is rather poor and it is evident that the experimentally

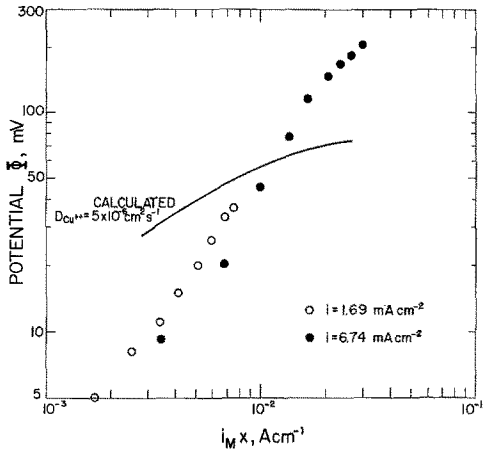

Fig. 8. Comparison of the measured and predicted potential difference Φ at various distances inside the cell.

measured potential gradient is much higher than the predicted one.

The fact that the measured concentrations are much lower than those predicted for any reasonable value of $D_{Cu^{2+}}$ indicates that the effective rate of mass transfer under our experimental conditions is actually larger than predicted, i.e., the rates of ionic diffusion and/or ionic migration must be larger than the values which result from solving the model equations. Notice that the experimentally measured potential gradient is several-fold greater than that calculated. This is obviously due to the effects of ionic interactions in the relatively concentrated electrolyte which have not been included in the equations of the model (notice also a similar effect in Fig. 6). Since the rate of ionic migration depends on the potential gradient, cf. Equation 2, for the same current, i.e., the same overall rate of mass transfer, an increase in the potential gradient $d\Phi/dx$ can only be possible if either the concentration of the metal ion and/or its gradient decrease. Consequently, the concentration of Cu^{2+} ions at any distance must be lower than that predicted (on the basis of a much lower potential gradient). A more quantitative interpretation of this behaviour can be obtained if one takes proper account of the effects of ionic interactions in the formulation of the model equations. This is beyond the scope of the present work.

After steady state was reached (with i = 6.74 mA cm^{-2}), the solution in the cell ($\sim$ 1.2 cm^3) was quantitatively transferred and diluted with water to 10 cm^3. The pH of the resulting solution was 1.7, whereas the pH of an equal volume of bulk solution after dilution to 10 cm^3 was 0.85. The predicted value is 1.89, as obtained by graphical integration of Equation 10. This decrease in H^+-ion concentration agrees with the predictions of the model and is due to ionic migration in accordance with the prevailing potential profile.

5. Conclusions

A model has been proposed to describe the transport of the various ionic species in the diffusion layer of a dissolving metal anode. The equations include transport of the metal ions and those of the supporting electrolyte by ionic diffusion and migration. The solutions show that the concentration of the supporting electrolyte is non-uniform throughout the diffusion layer. The implications of this non-uniformity have been assessed with regard to: (a) the ranges of current, distance, ionic charge and bulk electrolyte concentration for which ionic migration may or may not be ignored, (b) the measurement of electrochemical reaction order, and (c) the local variations of electrolyte resistivity within the diffusion layer.

The effects of current, metal-ion diffusivity, bulk concentration and ionic charge on the profiles of electrical potential and ionic concentrations have been evaluated. A dimensionless group, including all of these controlling parameters, $I = ix/zFc^0D_{Mz+}$, was developed. It is shown that the ratio R of the ionic migration flux to the molecular diffusion flux increases with increasing z, all other parameters being the same. The limiting value of this ratio R_{lim} was found to be simply equal to the charge on the metal ion z. This limit is obtained at $I = ix/zFc^0D_{mz+} > 10$. On the other hand, ionic migration becomes negligible ($R < 0.1$) for $I < 0.025$ for $z = 3$.

The major conclusion obtained from comparing the model predictions and the experimental results is that ionic interactions (at high electrolyte concentrations) produce larger-than-predicted potential gradients. Consequently, the concentration of the metal ions at a certain distance in the diffusion layer is lower than predicted.

These results complement and expand upon those for transport at planar surfaces existing in the literature [1–4] which are only for cathodic deposition. They also extend the treatment of pitting corrosion [14] to $z > 1$.

References

[1] K. Vetter, 'Electrochemical Kinetics', Academic Press, New York (1967) p. 169.
[2] V. G. Levich, 'Physico-Chemical Hydrodynamics', Prentice-Hall, Englewood Cliffs, N.J. (1962) p. 293.
[3] J. Newman in 'Advances in Electrochemistry and Electrochemical Engineering', Vol. 5, (edited by C. Tobias) John Wiley, New York (1967) p. 87.
[4] *Idem*, 'Electrochemical Systems', Prentice-Hall, Englewood Cliffs, N.J. (1973) p. 357.
[5] E. McCafferty and N. Hackerman, *J. Electrochem. Soc.* **119** (1972) 999.
[6] N. A. Darwish, F. Hilbert, W. J. Lorentz and H. Rosswag, *Electrochim. Acta* **18** (1973) 421.
[7] G. Bech-Nielsen, *ibid* **16** (1971) 849.
[8] *Idem, ibid* **19** (1974) 821.
[9] *Idem, ibid* **20** (1975) 619.
[10] *Idem, ibid* **21** (1976) 627.
[11] J. Bessane, L. Karakaya, P. Lorbeer and W. J. Lorentz, *ibid* **22** (1977) 1147.
[12] R. C. V. Piatti, A. J. Arvia and J. J. Podesta, *ibid* **14** (1969) 541.
[13] K. Kojima and C. W. Tobias, *J. Electrochem. Soc.* **120** (1973) 1026.
[14] H. W. Pickering and R. P. Frankenthal, *ibid* **119** (1972) 1297.
[15] B. G. Ateya and L. G. Austin, *ibid* **120** (1973) 1216.
[16] B. G. Ateya and H. W. Pickering, in 'Hydrogen in Metals', (edited by I. M. Bernstein and A. W. Thompson) ASM, Metals Park, Ohio (1974) p. 207.
[17] *Idem, J. Eleetrochem. Soc.* **122** (1975) 1018.
[18] D. A. Vermilyea and C. S. Tedmon, Jr, *ibid* **117** (1970) 437.
[19] R. Alkire, D. Ernsberger and D. Damon, *ibid* **123** (1976) 458.
[20] A. Emanuel and D. R. Olander, *J. Chem. Eng. Data* **8** (1963) 31.
[21] G. Jander and H. Möhr, *Z. Phys. Chem.* **A190** (1942) 81.
[22] *Idem, ibid* **37** (1943) 3320.
[23] A. I. Vogel, 'Textbook of Quantitative Inorganic Analysis' 3rd edn, John Wiley, New York (1962).